Long-term evolution of upper stratospheric ozone at selected stations of the Network for the Detection of Stratospheric Change (NDSC)

W. Steinbrecht,[1] H. Claude,[1] F. Schönenborn,[1] I. S. McDermid,[2] T. Leblanc,[2] S. Godin,[3] T. Song,[3] D. P. J. Swart,[4] Y. J. Meijer,[4] G. E. Bodeker,[5] B. J. Connor,[5] N. Kämpfer,[6] K. Hocke,[6] Y. Calisesi,[6,7] N. Schneider,[8] J. de la Noë,[8] A. D. Parrish,[9] I. S. Boyd,[10] C. Brühl,[11] B. Steil,[11] M. A. Giorgetta,[12] E. Manzini,[13] L. W. Thomason,[14] J. M. Zawodny,[14] M. P. McCormick,[15] J. M. Russell III,[15] P. K. Bhartia,[16] R. S. Stolarski,[16] and S. M. Hollandsworth-Frith[16]

[1] The long-term evolution of upper stratospheric ozone has been recorded by lidars and microwave radiometers within the ground-based Network for the Detection of Stratospheric Change (NDSC), and by the space-borne Solar Backscatter Ultra-Violet instruments (SBUV), Stratospheric Aerosol and Gas Experiment (SAGE), and Halogen Occultation Experiment (HALOE). Climatological mean differences between these instruments are typically smaller than 5% between 25 and 50 km. Ozone anomaly time series from all instruments, averaged from 35 to 45 km altitude, track each other very well and typically agree within 3 to 5%. SBUV seems to have a slight positive drift against the other instruments. The corresponding 1979 to 1999 period from a transient simulation by the fully coupled MAECHAM4-CHEM chemistry climate model reproduces many features of the observed anomalies. However, in the upper stratosphere the model shows too low ozone values and too negative ozone trends, probably due to an underestimation of methane and a consequent overestimation of ClO. The combination of all observational data sets provides a very consistent picture, with a long-term stability of 2% or better. Upper stratospheric ozone shows three main features: (1) a decline by 10 to 15% since 1980, due to chemical destruction by chlorine; (2) two to three year fluctuations by 5 to 10%, due to the Quasi-Biennial Oscillation (QBO); (3) an 11-year oscillation by about 5%, due to the 11-year solar cycle. The 1979 to 1997 ozone trends are larger at the southern mid-latitude station Lauder (45°S), reaching −8%/decade, compared to only about −6%/decade at Table Mountain (35°N), Haute Provence/Bordeaux (≈45°N), and Hohenpeissenberg/Bern(≈47°N). At Lauder, Hawaii (20°N), Table Mountain, and Haute Provence, ozone residuals after subtraction of QBO- and solar cycle effects have levelled off in recent years, or are even increasing. Assuming a turning point in January 1997, the change of trend is largest at southern mid-latitude Lauder, +11%/decade, compared to +7%/decade at northern mid-latitudes. This points to a beginning recovery of upper stratospheric ozone. However, chlorine levels are still very high and ozone will remain vulnerable. At this point the most northerly mid-latitude station, Hohenpeissenberg/Bern differs from the other stations, and shows much less clear evidence for a beginning recovery, with a change of trend in 1997 by only +3%/decade. In fact, record low upper stratospheric ozone values were observed at Hohenpeissenberg/Bern, and to a lesser degree at Table Mountain and Haute Provence, in the winters 2003/2004 and 2004/2005.

---

[1]German Weather Service, Hohenpeissenberg, Germany.
[2]Table Mountain Facility, NASA-JPL, Wrightwood, California, USA.
[3]CNRS Service d'Aeronomie, Paris, France.
[4]RIVM, Bilthoven, Netherlands.
[5]NIWA, Omakau, Central Otago, New Zealand.
[6]Institute of Applied Physics, University of Bern, Bern, Switzerland.
[7]Now at International Space Science Institute, Bern, Switzerland.

[8]OASU/L3AB, Université Bordeaux 1, CNRS-INSU, Floirac, France.
[9]Astronomy Department, University of Massachusetts, Amherst, Massachusetts, USA.
[10]NIWA-ERI, Ann Arbor, Michigan, USA.
[11]Max-Planck-Institute for Chemistry, Mainz, Germany.
[12]Max-Planck-Institute for Meteorology, Hamburg, Germany.
[13]Istituto Nazionale di Geofisica e Vulcanologia, Bologna, Italy.
[14]NASA LARC, Hampton, Virginia, USA.
[15]Hampton University, Hampton, Virginia, USA.
[16]NASA GSFC, Greenbelt, Maryland, USA.

1. Introduction

[2] Ozone in the upper stratosphere at mid-latitudes has been declining by about 15% over the last two decades [*SPARC*, 1998; *WMO*, 2003]. This decline has been predicted and is caused by catalytic ozone destruction through chlorine, which is released in the stratosphere from anthropogenic Chloro-Fluoro-Carbons (CFCs) [*Crutzen*, 1974; *Molina and Rowland*, 1974]. As expected, the largest relative ozone changes have occurred at approximately 40 km altitude [*WMO*, 2003]. Natural variations of ozone in this altitude range come from the Quasi-Biennial Oscillation of equatorial zonal winds (QBO) [*Zawodny and McCormick*, 1991; *Leblanc and McDermid*, 2001], and from the 11-year solar cycle [*Hood et al.*, 1993]. Additional factors influencing upper stratospheric ozone are variations in temperature [*Douglass et al.*, 1985; *Rosenfield et al.*, 2002], solar proton events [*Jackman et al.*, 1999], variations in the global meridional circulation [*Salby et al.*, 2002], and changes in water vapour, methane or nitrous oxides [*WMO*, 1999; *Li et al.*, 2002; *Randeniya et al.*, 2002].

[3] After 1987, the emission of harmful CFCs has been phased out in response to the International Montreal Protocol and its later amendmends. These international agreements were very successful: Chlorine loading of the upper stratosphere seems to have peaked sometime between 1997 and 2002, about 6 years after the tropospheric maximum [*Anderson et al.*, 2000; *WMO*, 2003; *Rinsland et al.*, 2003]. However, compared to the fast increase since the late 1970s, the decline of chlorine will be slow. A return to the chlorine levels of 1980 is not expected before 2050 or 2060 [*Engel et al.*, 2002; *WMO*, 2003]. Recently, it has been discussed whether positive effects of the now slightly decreasing chlorine levels can already be seen in upper stratospheric ozone [*Newchurch et al.*, 2003]. Such a "beginning recovery" is not easily separated from ozone increases related to the recent maximum of the 11-year solar cycle [*Steinbrecht et al.*, 2004].

[4] The purpose of this paper is to present some main results of the long-term ozone monitoring carried out within the framework of the international Network for the Detection of Stratospheric Change (NDSC, http://www.ndsc.ws) by several ground-based lidar (laser-radar) and microwave radiometer instruments. These measurements started in the late 1980s and early 1990s. We focus on those NDSC stations with the longest and least interrupted records of ozone between 35 and 45 km altitude. Note that this altitude range is not covered by standard balloon-borne ozonesondes. The stations used are given in Table 1. For the purpose of this study, the nearby sites Hohenpeissenberg/Bern and Haute Provence/Bordeaux are considered as one station, respectively. More information about the stations and instruments is given by *Claude et al.* [1994], *Guirlet et al.* [2000], *Leblanc and McDermid* [2000], *Tsou et al.* [2000], *Calisesi et al.* [2001], *Brinksma et al.* [2002], *Schneider et al.* [2003], and *Godin-Beekmann et al.* [2003].

[5] The NDSC data are compared to three long-term satellite data sets: The 1979 to 2003 data set from

various Solar Backscatter Ultraviolet instruments (SBUV) [*Hilsenrath et al.*, 1995; *Bhartia et al.*, 1996], the 1979 to 2004 data set from the Stratospheric Aerosol and Gas Experiment I and II (SAGE) [*McCormick et al.*, 1989], and the 1991 to 2004 data set from the HALogen Occultation Experiment (HALOE) [*Russell et al.*, 1993].

[6] Further, results are presented from a 1960 to 1999 model simulation carried out with the fully coupled Middle Atmosphere European Center/Hamburg version 4 chemistry-climate model (MAECHAM4-CHEM) [*Steil et al.*, 2003; *Manzini et al.*, 2003]. A comparison of MAECHEM4-CHEM with other chemistry climate models is reported in *Austin et al.* [2003]. Chemistry climate models are the main tools for predicting the future of the ozone layer. Therefore, it is important to evaluate their performance in the past. Here we take advantage of the availability of a "transient" simulation from MAECHAM4-CHEM, called ECHAM hereafter. This simulation includes effects from increasing greenhouse gases and total chlorine (CO_2, N_2O, CH_4, NO_x, and $CFCs$), the 11-year solar cycle, an assimilated QBO, and volcanic aerosol from the Agung (1963), El-Chichon (1982), and Pinatubo (1991) eruptions. Observed variations in sea surface temperatures and ice conditions are prescribed as well. In part because of the lack of a continuing consistent data set for these latter boundary conditions, the simulation ends in 1999, unfortunately, and has not yet been extended.

[7] The present paper extends previous studies, which relied on the SAGE and HALOE data only [*SPARC*, 1998; *Newchurch et al.*, 2003; *Cunnold et al.*, 2004]. For the long-term variations, we follow the approach of a previous study [*Steinbrecht et al.*, 2004], which considered data for Hohenpeissenberg only. We present additional stations and new observations from the years 2003 to 2005.

2. Techniques and Data

2.1. Differential Absorption Lidar

[8] For observing upper stratospheric ozone, most NDSC stations use either Differential Absorption Lidar (DIAL) or microwave radiometer systems. DIAL systems measure the ozone absorption of an atmospheric layer by comparing atmospheric return signals from the top and bottom of the layer, at two (or more) wavelengths [*Pelon and Mégie*, 1982]. Ozone number density is derived from the measured ozone absorption. One wavelength, usually 308 nm, is absorbed by ozone, whereas another wavelength, usually 353 or 355 nm, is absorbed much less and serves as a reference for the rest of the atmosphere without ozone. The measurement is differential in wavelength and in altitude, which makes it self-calibrating and ideally suited for long-term purposes [*Werner et al.*, 1983; *McDermid et al.*, 1990]. A summary of many validation exercises within the NDSC framework [*Keckhut et al.*, 2004] shows that the accuracy of a typical stratospheric ozone profile measured by lidar is approximately 3% at 35 km, and 10% at 40 km, depending on averaging time, system power, and other factors [see also *McDermid et al.*, 1998; *McPeters et al.*, 1999]. Altitude

Table 1. NDSC Stations and Instruments Used in This Investigation[a]

Name	Latitude, °N	Longitude, °E	Instrument
Hohenpeissenberg/Bern	47.8/47.0	11.0/7.5	L/M
Haute Provence/Bordeaux	43.9/44.8	5.7/−0.5	L/M
Table Mountain	34.5	−117.7	L
Mauna Loa, Hawaii	19.5	−155.6	L, M
Lauder	−45.0	169.7	L, M

[a]L, lidar; M, microwave. Hohenpeissenberg/Bern, and Haute Provence/Bordeaux, are considered as one station.

resolution is of the order of 1 km at 30 km altitude and 5 km at 40 km [*Godin et al.*, 1999; *Keckhut et al.*, 2004]. Precision and altitude resolution become poorer with increasing altitude. Most systems do not provide reliable data above 50 to 55 km. Lidars need clear nights for their measurements, but this has not been a relevant drawback for long-term monitoring. For this study, the lidar (and microwave radiometer) data were obtained from the database of the Network for the Detection of Stratospheric Change (NDSC) (ftp://ndsc.ncep.noaa.gov), or directly from the stations.

2.2. Solar Occultation

[9] SAGE and HALOE measure the ozone absorption at different altitudes by comparing solar spectra taken at different (high and low) paths through the earth's atmosphere, as the sun is setting or rising for the satellite (solar occultation). SAGE uses the visible part of the spectrum (Chappuis band centered at 600 nm) [*McCormick et al.*, 1989], whereas HALOE uses infrared absorption at about 9.6 μm [*Russell et al.*, 1993]. Slant path absorption is obtained by comparing the spectra with the reference spectrum taken above the atmosphere at each sunrise/sunset. The vertical resolution of the obtained profile is 0.5 to 2 km, and the accuracy is better than 5 to 10% between 20 to 50 km altitude. The measurement principle is self-calibrating and long-term stability can be achieved. A disadvantage is that measurements can only be taken at locations and times where the sun sets or rises relative to the spacecraft. For a typical mid-latitude location, measurements are more frequent in winter, but can be quite rare in summer. For the month of August, for example, SAGE II took only 59 measurements during the entire 1985 to 2004 period in a ±7.5° latitude and ±15° longitude box around Hohenpeissenberg, compared to 160 profiles measured by the lidar. For January, the corresponding numbers are 339 profiles for SAGE and 139 for the lidar. For HALOE, in the entire 1992 to 2004 period, the numbers are 189 profiles in January, but only 8 profiles in June.

[10] SAGE II (V6.20) and HALOE (V19) data were obtained from ftp://ftp-rab.larc.nasa.gov/pub/sage2/v6.20 and http://haloedata.larc.nasa.gov. For the climatological comparisons in section 3 we used mean profiles from data obtained within ±7.5° latitude and ±15° longitude boxes centered at the stations geolocations. For the long-term evolution in section 4, however, we used zonal means over 10° latitude bands centered at 45°S, 35°S, 25°S, and so on, every 10° up to 45°N, and interpolated to the stations latitudes. Corresponding zonal means for SAGE I were provided by M. Newchurch (private communication,

2004). These SAGE I data are adjusted following the recommendations from *Wang et al.* [1996]. SAGE data contaminated by heavy stratospheric aerosol loading, particularly after the Mt. Pinatubo eruption in 1991 were excluded using the criteria given by *Wang et al.* [1996, 2002].

2.3. Backscattered Ultraviolet

[11] SBUV instruments measure incoming solar irradiance and nadir radiance backscattered by the atmosphere at several wavelengths in the ultraviolet [*Heath et al.*, 1975]. The ratio between incoming and backscattered radiation carries information about the amount of ozone in the atmosphere. Because radiation at the shorter wavelengths is absorbed by ozone higher in the atmosphere than radiation at the longer wavelengths, the use of different wavelengths allows for a measure of the ozone profile [*Bhartia et al.*, 1996]. Measurements can be taken over the sunlit portion of the globe and are very frequent. Altitude resolution is about 10 km and is coarser than for lidar, SAGE or HALOE. An accuracy of 5 to 10% is reached in the stratosphere. SBUV measurements are not self-calibrating. Maintaining a consistent calibration over many years and many instruments is a substantial task [*Hilsenrath et al.*, 1995; *Bhartia et al.*, 1996]. Here we used the 5° zonal mean Version 8.0 data from http://code916.gsfc.nasa.gov/Data_services/merged/mod_data.public.html. In this data set, results from 4 different SBUV instruments are merged and adjusted in order to calibrate all instruments to a common standard [*Frith et al.*, 2004].

2.4. Microwave Radiometers

[12] Microwave radiometers record emission spectra from thermally induced rotational transitions of atmospheric ozone, typically around 110 or 142 GHz [*Parrish et al.*, 1992; *Kämpfer*, 1995; *Connor et al.*, 1995; *Schneider et al.*, 2003]. Since the recorded transition lines are broadened by pressure, the recorded line shape contains information on the vertical distribution of ozone. Radiation at the wings of the spectra carries information about ozone at low altitudes (=high pressures), while radiation at wavelengths close to the line center results from emission originating at all altitudes (=all pressures) along the instrument's line of sight. A big advantage is that ground-based microwave radiometers are fairly independent of weather conditions and take measurements around the clock, with a typical time resolution of one or two hours. Altitude resolution and accuracy of the retrieved stratospheric ozone profiles are 7 to 10 km and 7 to 10%, respectively. Many studies have validated ozone profiles from microwave radiometers [e.g., *McDermid et al.*, 1998; *McPeters et al.*, 1999; *Tsou et al.*, 2000].

2.5. Chemistry Climate Model

[13] The Middle Atmosphere European Center/Hamburg version 4 Chemistry-climate model is based on the full coupling of the general circulation model MAECHAM4 with the chemistry model CHEM [*Steil et al.*, 2003; *Manzini et al.*, 2003]. MAECHAM4 covers the global (3-D) atmosphere and extends from the surface to 0.01 hPa (80 km). The resolution used is the T30 horizontal truncation with 39 vertical levels. In MAECHAM4, gravity wave

effects in the mesosphere, of fundamental importance for a realistic representation of middle atmosphere dynamics including the Brewer-Dobson circulation, are parameterized [*Manzini and McFarlane*, 1998]. CHEM simulates the photochemical processes relevant to stratospheric ozone, including heterogeneous chemistry. Trace gas concentrations from CHEM are fed back into the radiative scheme of MAECHAM4 [*Steil et al.*, 2003]. Here we use upper stratospheric ozone results from a 1960 to 1999 simulation, in which the effects of increasing chlorine and greenhouse gases ($CFCs$, CO_2, N_2O, CH_4, and NO_x) [*WMO*, 2003], observed variations in sea surface temperatures and ice-coverage [*Rayner et al.*, 2003], a nudged QBO [*Giorgetta and Bengtsson*, 1999], volcanic aerosol from the major eruptions in 1963, 1982 and 1991 [*Timmreck et al.*, 2004], and the 11-year solar cycle [*Tourpali et al.*, 2003] are all accounted for. The full coupling and the external forcings applied in this simulation result in a realistic evolution of the main trace gases. Unfortunately, the simulation ends in 1999, and has not yet been extended into the 21st century.

3. Climatological Means

[14] Next, a brief description of some general climatological features is given. The purpose is not to introduce a new ozone climatology. Rather, an overview of some main features is given. Systematic differences in the climatologies recorded by the different instruments are described. By comparing climatologies we take a somewhat different approach than typical instrument comparisons. Typical instrument comparisons use only a subset of profiles, usually selected to match well in space and time, and often measured under special conditions. This subset can sometimes be very small. It might also not be representative for routine observations. By comparing climatologies, a very large number of routine profiles is used, albeit at the expense of possible mismatches. However, rather than a selected subset the operational "end-product" is compared, i.e., the atmospheric record provided by each data set. Here we consider climatological differences as a reasonable proxy for systematic differences between data sets or instruments.

3.1. Annual Cycle

[15] The average annual cycle of ozone number density, recorded by the various data sets, is shown in Figure 1 for three selected altitudes in the stratosphere. This average annual cycle was obtained by first averaging all available monthly mean profiles from the period 1993 to 2003, separately for each month of the year, each station and each data set. For SAGE and HALOE, only profiles taken within ±7.5° latitude and ±15° longitude of the stations were considered. For ECHAM, the profiles from the grid-point closest to each station were taken. This gives climatological mean profiles for each month of the year and each data set and station. For Figures 1a and 1b the climatological mean profiles were averaged over all Northern Hemisphere stations, in a second step. Results for Lauder, which is situated in the Southern Hemisphere and has a quite different annual cycle, are shown in Figures 1c and 1d. 1993 to 2003 was chosen as the reference period, because all data sources

cover a large part of this period, and ozone values were fairly constant over this period (compare Figure 4). SBUV and Bordeaux microwave radiometer data were not available as number density versus altitude profiles and are not included in Figure 1. See *SPARC* [1998], *Tsou et al.* [2000], *Schneider et al.* [2003], or *Nazaryan and McCormick* [2005] for a comparison of SBUV or microwave data to other instruments.

[16] The annual cycles depicted in Figure 1 follow well known characteristics: In the lower stratosphere, e.g., at 20 km altitude, the highest ozone levels occur in late winter, February to March (August or September for Lauder), the lowest ozone levels in late summer, August (or February for Lauder). This is a consequence of the annual cycle of the global meridional Brewer-Dobson circulation, which is strongest in late winter and weakest in fall. The Brewer-Dobson circulation transports ozone rich air to high latitudes and lower altitudes, particularly in late winter. Its annual cycle produces the observed total column ozone maximum in late winter, and the minimum in late summer [e.g., *Brasseur and Solomon*, 1984].

[17] In the middle stratosphere, e.g., at 35 km altitude, ozone peaks in late summer, July or August, for the Northern Hemisphere stations, but in late spring, October or November, for Lauder in the Southern Hemisphere. The general shape of the annual cycle at 35 km reflects the photochemical production of ozone by sunlight, i.e., high in summer, and low in winter. Note, however, that for the Northern Hemisphere stations there is a time lag between the highest solar elevation in June and the ozone maximum in August (July for the ECHAM model). At Lauder, ozone peaks at 35 km in October or November, before the highest solar elevation in December. In the upper stratosphere at 45 km, these differences between the hemispheres are much more pronounced. In the Northern Hemisphere, ozone peaks in late summer, August or September, similar to 35 km. The ozone buildup during spring and summer is rather slow, while the ozone decline in fall is quite fast.

[18] At Lauder, however, the annual cycle at 45 km is quite different. There is only a small late summer peak in March, but an additional very large ozone peak in spring, September or October (Figures 1c and 1d). The exact shape of the annual cycle is obviously determined not only by solar irradiation. It is also affected very much by the way in which the various chemical production and loss mechanisms react to the annual cycles of temperature and other trace gases. The tropical stratopause semi-annual oscillation, the changing Brewer-Dobson circulation, and light absorption at higher levels are also important [*Brasseur and Solomon*, 1984; *Schneider et al.*, 2005]. The large spring peak in the Southern Hemisphere at 45 km is largely caused by slowing ozone loss cycles due to the colder winter temperatures of the Southern Hemisphere. Reduced transport due to the stronger Southern Hemisphere winter vortex and a weaker Brewer/Dobson circulation also plays a role [e.g., *Li et al.*, 2002].

[19] In Figure 1 the observed annual cycles from all the observations agree closely. While following the same general cycles, the ECHAM model results show, however, characteristic differences: In the lower stratosphere (20 km) ECHAM ozone values are ≈25% higher than observed. This is due to unrealistically fast vertical transport in
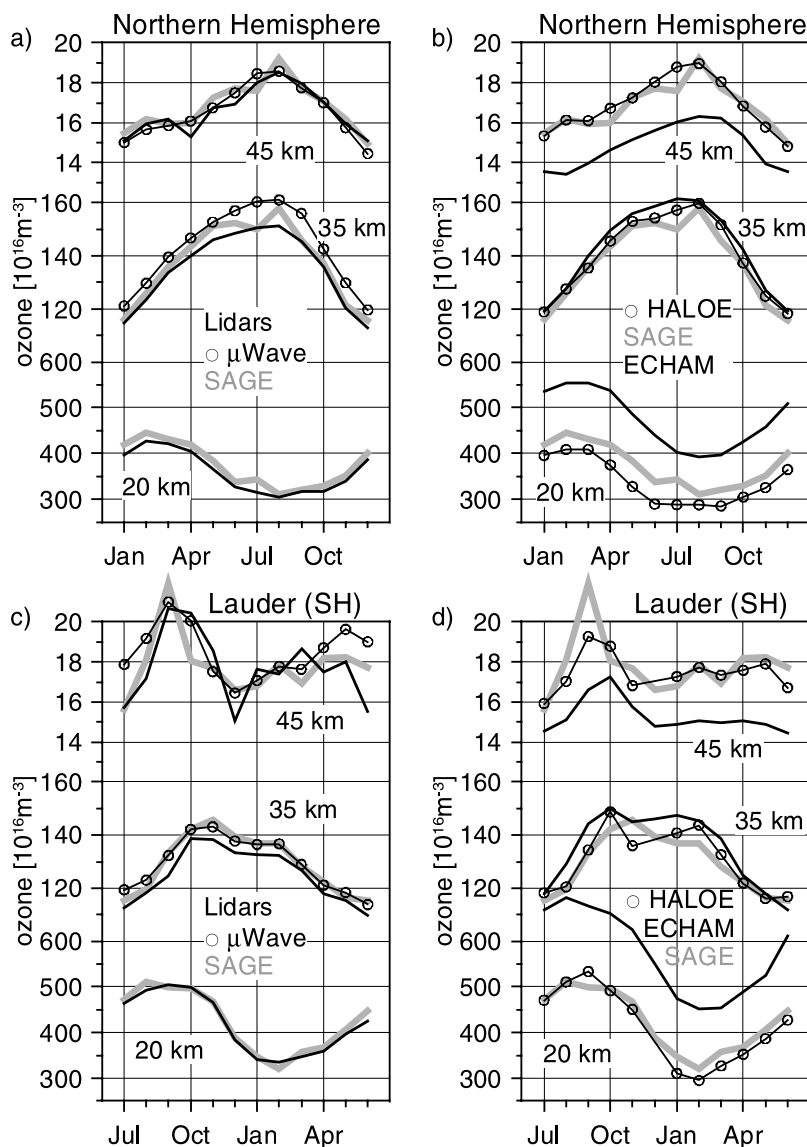
Figure 1. Annual cycle of ozone number density reported by the different instruments over the 1993 to 2003 period. (a) and (b) Results are averaged over the Northern Hemisphere NDSC stations Hohenpeissenberg/Bern, Haute Provence, Table Mountain and Hawaii. (c) and (d) Results for Lauder, in the Southern Hemisphere. Figures 1a and 1c show results for SAGE, lidars and microwave. Figures 1b and 1d show results for SAGE, HALOE and the MAECHAM4-CHEM simulation. Bordeaux microwave and SBUV data were not included. For SAGE and HALOE, only profiles within ±7.5° latitude and ±15° longitude of each station were considered. For MAECHAM4-CHEM, data from the grid-point nearest to each station were used.

ECHAM [*Steil et al.*, 2003]. Too much ozone-rich air is transported down at model levels below the ozone mixing ratio maximum, resulting in too high ECHAM ozone values below about 35 km. In the upper stratosphere above 37 km, on the other hand, ECHAM simulates ozone values lower than observed, e.g., by 12% at 45 km. At these altitudes ozone at mid- and low-latitudes is mostly under photochemical control. In a recent chemistry climate model validation exercise, too low methane and too high *ClO* concentrations were reported in the upper stratosphere for MAECHAM4-CHEM. This results in enhanced chemical ozone destruction in the upper stratosphere, and can largely explain the

low ozone values simulated by MAECHAM4-CHEM above 37 km.

3.2. Difference Profiles

[20] The vertical profile of the climatological mean difference between the various data sources and SAGE II is given in Figure 2. SAGE II is used as the reference here, because it's principle is self-calibrating, and it provides a near-global and very long-term data set, that lies well within the range of the other observations. This makes it most suited as a reference, but does not imply that SAGE data are closer to the truth than data from the other instruments. For Figure 2, climatological monthly mean differences between
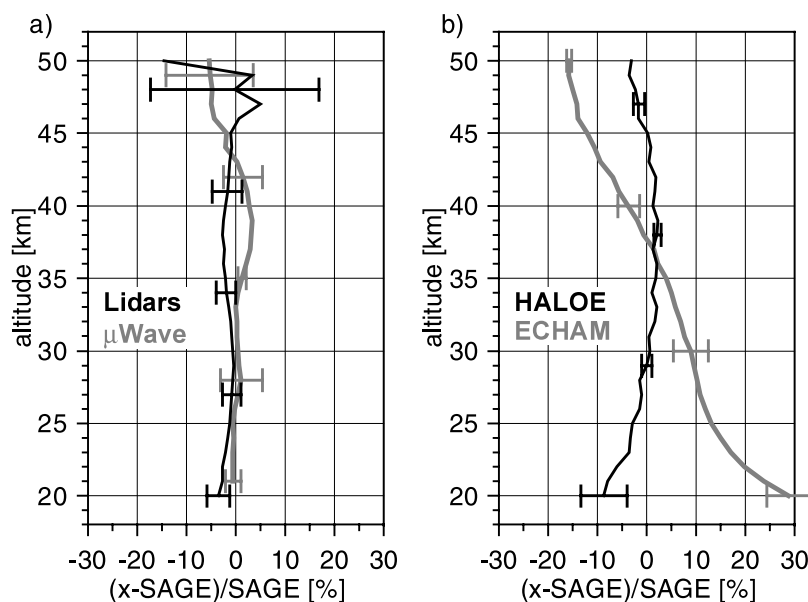
Figure 2. Average deviation of climatological annual mean profiles obtained by individual instruments from the mean profile by SAGE. Climatologies are over the period from 1993 to 2003. Results are averaged over the respective NDSC stations from Table 1. Error bars give the 1σ standard deviation between stations. (a) Results for lidars and microwave radiometers versus SAGE. (b) Results for HALOE and MAECHAM4-CHEM simulation versus SAGE.

SAGE and the other data sources were first averaged over the year, then over the different stations. The error bars give the 1σ standard deviation between stations. At most altitudes between 20 and 50 km the climatological mean profiles observed by the different instruments are within ±5% of the climatological mean SAGE profile. Overall, Figure 2 demonstrates a high level of consistency between the various ground-based and satellite-based instruments. Note that due to diurnal variations of ozone above about 40 km [*Huang et al.*, 1997], systematic differences of 1 or 2% have to be expected at the upper altitudes between SAGE/HALOE which measure at sunrise and sunset, the lidars, which measure at night, and the 24 hour microwave measurements. As expected from Figure 1, ECHAM shows substantially higher values than the observations below about 37 km altitude and substantially lower values above (Figure 2b).

[21] Small but consistent biases, both over the year and between stations, are seen in Figure 2b between SAGE and HALOE: HALOE ozone values tend to be up to 3% higher than SAGE values between 30 and 45 km, but 10% lower than SAGE at 20 km and 5% lower at 50 km. These differences are seen consistently at all stations, and throughout the year. Lower HALOE than SAGE values below 30 and above 45 km, as well as higher HALOE than SAGE values between 30 and 42 km, have been reported before [*SPARC*, 1998; *Morris et al.*, 2002; *Nazaryan et al.*, 2005].

[22] The lidars also exhibit small but consistent differences to SAGE: Below 25 km, most lidars tend to be systematically lower than SAGE, by up to 5%. To some degree, this is a consequence of the fact that the lidars tend to measure more often during tropospheric high pressure situations, when clear nights are more frequent, than during

low pressure situations, when clear nights are rarer. Since ozone values in the lower stratosphere are lower during tropospheric high pressure [*DeBacker et al.*, 1994; *Steinbrecht et al.*, 1998], this leads to a meteorological low bias of the lidar ozone data at some stations and at altitudes below 25 km. For Hohenpeissenberg, this bias can reach 5% at 20 km. Between 30 and 45 km, the lidars also tend to give a few percent lower ozone values, on average, than SAGE. This minor bias may partly be due to a diurnal cycle of 1 or 2% higher ozone values around 40 km at sunset/sunrise, when SAGE measures, compared to during the night, when the lidars measure [*Huang et al.*, 1997]. A good part of the bias, however, must also be attributed to the lidar systems and the specific processing used at the stations (see, e.g., Hohenpeissenberg in Figure 3).

[23] Unlike SAGE, HALOE, or MAECHAM4-CHEM, which use the same processing algorithm over the globe, hardware and processing algorithms for lidars or microwave radiometers can differ from station to station. To give more detail, Figure 3 shows difference profiles for the individual lidar and microwave stations. While all lidars in Figures 3a and 3b show very similar and minor differences to SAGE below 35 km, larger systematic deviations begin to appear above 35 km, particularly for the less powerful systems (Hohenpeissenberg and Haute Provence). The more powerful systems (Table Mountain, Mauna Loa) show almost no significant deviation up to 50 km altitude. The Hohenpeissenberg lidar shows systematically lower values by almost −10% at 39 km, and by more than −10% above 48 km. The Haute Provence lidar shows slightly higher values than SAGE above 35 to 40 km, up to +5% at 45 km. Similar systematic differences between lidars and SAGE were reported in Figure 2.14 of the *SPARC* [1998] assessment. These systematic differences are comparable to systematic
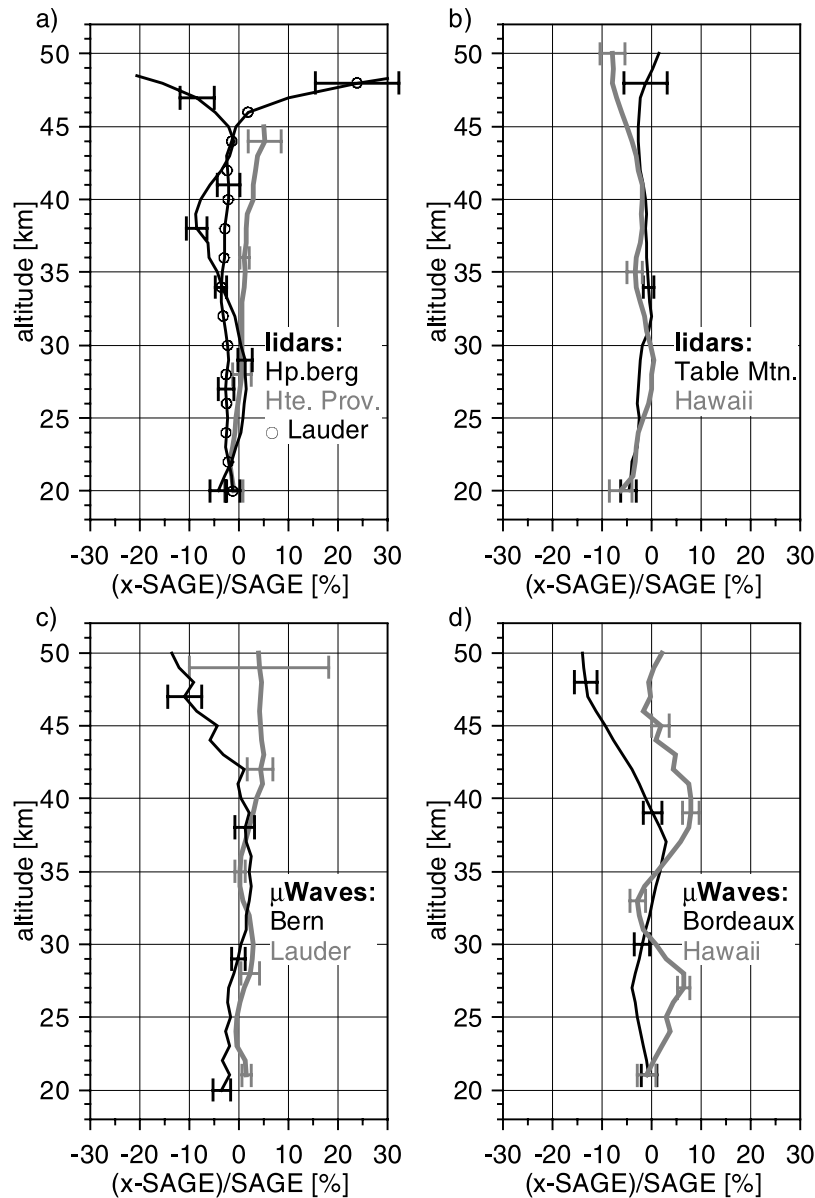
Figure 3. (a) and (b) Deviation of 1993 to 2003 climatological annual mean profiles obtained by lidars from climatological SAGE mean profile over this period. (c) and (d) Same for microwave radiometers and SAGE. Error bars give the 2σ standard deviation of the mean over the annual cycle. For the Bordeaux microwave radiometer, ozone number density versus altitude data were not available. Instead, the line for the Bordeaux microwave shows results of a comparison by *Schneider et al.* [2003], based on 137 coincident mixing ratio profiles from the years 1995 to 1998.

biases seen in tests of lidar processing algorithms [*Steinbrecht et al.*, 1997; *Godin et al.*, 1999].

[24] The microwave radiometers, on average, tend to give slightly higher ozone values than SAGE around 38 km, and slightly lower values above 45 km (Figure 2). The agreement between individual microwave radiometers and SAGE, shown in Figures 3c and 3d, is generally better than 5% below 45 km [see also *Connor et al.*, 1995; *McDermid et al.*, 1998; *McPeters et al.*, 1999]. Larger differences are seen for the microwave radiometer at Hawaii, operated by the same group as the Lauder radiometer, around 27 and 40 km altitude, and for the Bern and Bordeaux radiometers above 45 km. For the Bordeaux microwave radiometer,

number density versus altitude data were not available. Instead, we plotted the difference reported in *Schneider et al.* [2003], where 137 individual profiles from the years 1995 to 1998 were compared. The magnitude of the microwave to SAGE differences is comparable to what is seen for the lidars. Without going into detail, most of the larger deviations are attributed to the retrieval algorithms used at the various stations, the uncertainty in the conversion from mixing ratio versus pressure to number density versus altitude coordinates, and sampling differences [*Tsou et al.*, 2000; *Schneider et al.*, 2003; *Meijer et al.*, 2003]. The diurnal cycle of ozone above about 40 km altitude will
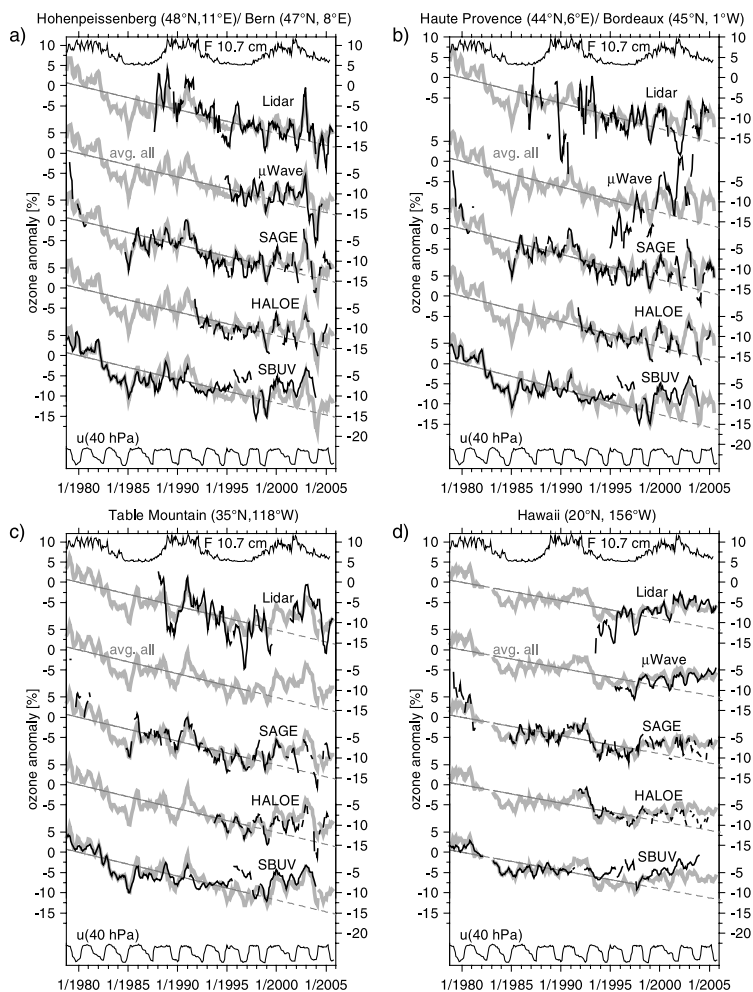
Figure 4. Ozone anomalies above the four Northern Hemisphere stations, averaged over the altitude range from 35 to 45 km. For SAGE, SBUV and HALOE zonal mean data are shown. Data are smoothed by a 5 month running mean. The underlaid thick grey line is the average anomaly record obtained by averaging all available instrumental records at each station. However, at Haute Provence/Bordeaux the microwave record and the very low lidar ozone values around 1990 were not included in the average. The grey trend line gives the 1979 to 1996 linear trend of the average record at each station, extrapolated after 1996. Thin curves at the top show the solar flux at 10.7 cm, a proxy for solar activity (ftp://ftp.ngdc.noaa.gov/STP/SOLAR_DATA/SOLAR_RADIO/FLUX/). Thin curves at the bottom give zonal wind anomalies at 40 hPa above Singapore, a proxy for the QBO (B. Naujokat, private communication, 2005). Bern microwave data are plotted in the Hohenpeissenberg panel, and Bordeaux microwave data are plotted in the Haute Provence panel.

likely also play a role. A detailed discussion of these matters is not within the scope of this paper.

4. Long-Term Variations

[25] In this section, our focus is on the evolution of upper stratospheric ozone anomalies since 1979. Anomalies are defined as the deviation of individual monthly means from the average climatological annual cycle. For best results, we applied the individual climatological cycle of each instrument at each station. Note that this procedure removes nearly all systematic differences between the data sets. For the stations from Table 1, the evolution of upper stratospheric ozone relative anomalies, averaged between 35 and 45 km altitude, is shown in Figures 4 and 5. For

plotting, the data were smoothed by a 5 month running mean. Hohenpeissenberg lidar and Bern microwave data (Figure 4a), as well as Haute Provence lidar and Bordeaux microwave data (Figure 4b) are plotted into common panels. For SBUV, the average relative anomaly of the 3 layers between 6.4 and 1.6 hPa ($\approx$34 to 45 km) is given. For all the satellite instruments we interpolated zonal means to the station latitudes. All records starting before 1990 clearly show the long-term decline of ozone in the upper stratosphere. In addition to the anomaly records from the individual instruments, an average anomaly record was obtained for each station by averaging the lidar, microwave, SAGE, HALOE and SBUV anomaly records available at this station. In all panels of Figures 4–9 these average records
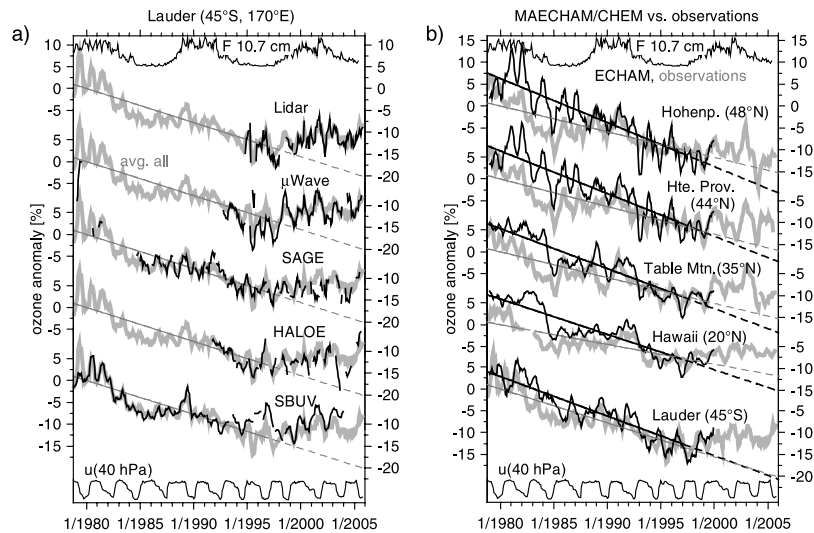
Figure 5. (a) Same as Figure 4, but for the southern mid-latitude station Lauder (New Zealand). (b) Average instrumental ozone anomaly record at the five stations (thick grey line) compared to the MAECHAM4-CHEM simulated record (black line). Data are smoothed by a 5 month running mean. The grey and black trend lines show the 1979 to 1996 linear trend of the average instrumental and MAECHAM4-CHEM simulated records, respectively. The dashed lines give the extrapolation of the trends after 1996.
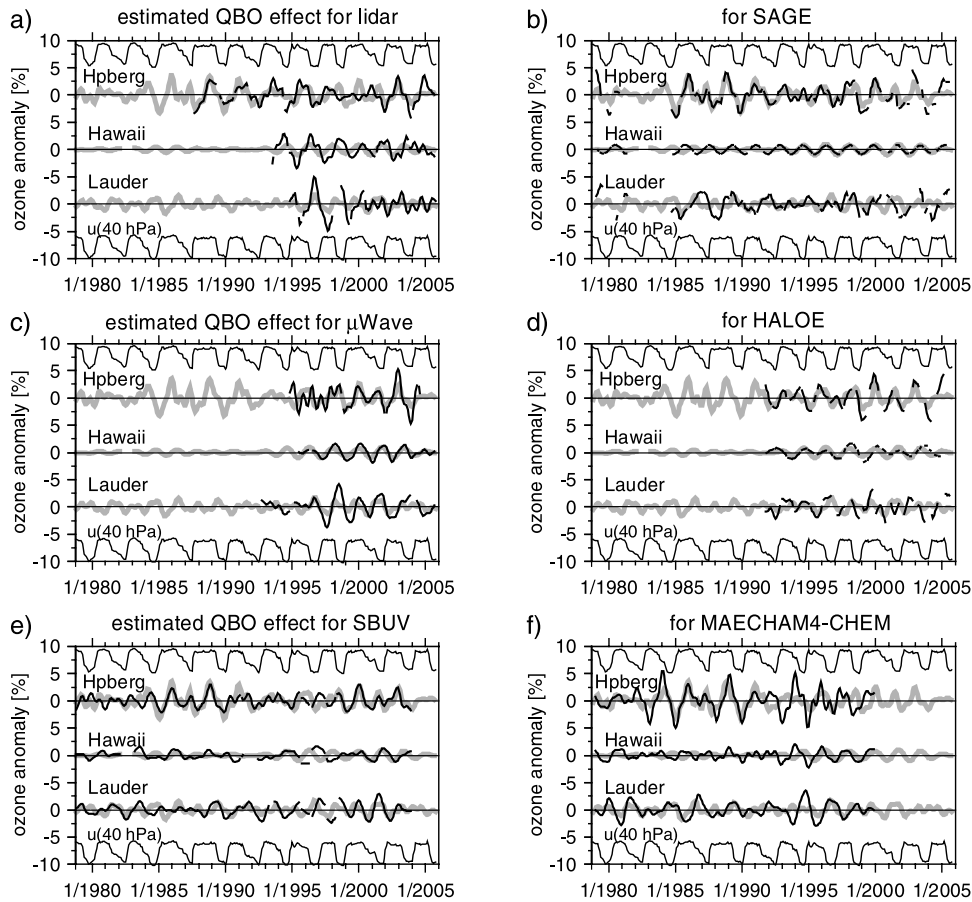

Figure 6. Estimates of ozone anomalies related to the QBO, for three selected stations. Note that the QBO estimate is for relative ozone anomalies, averaged from 35 to 45 km altitude. The different panels show results for the different data sets. Results for the all instrument average data set have been underlaid at each station (thick grey line). Thin curves at top and bottom give zonal wind anomalies at 40 hPa above Singapore. Figure 6f compares results for the MAECHAM4-CHEM simulation with the average observed data set.
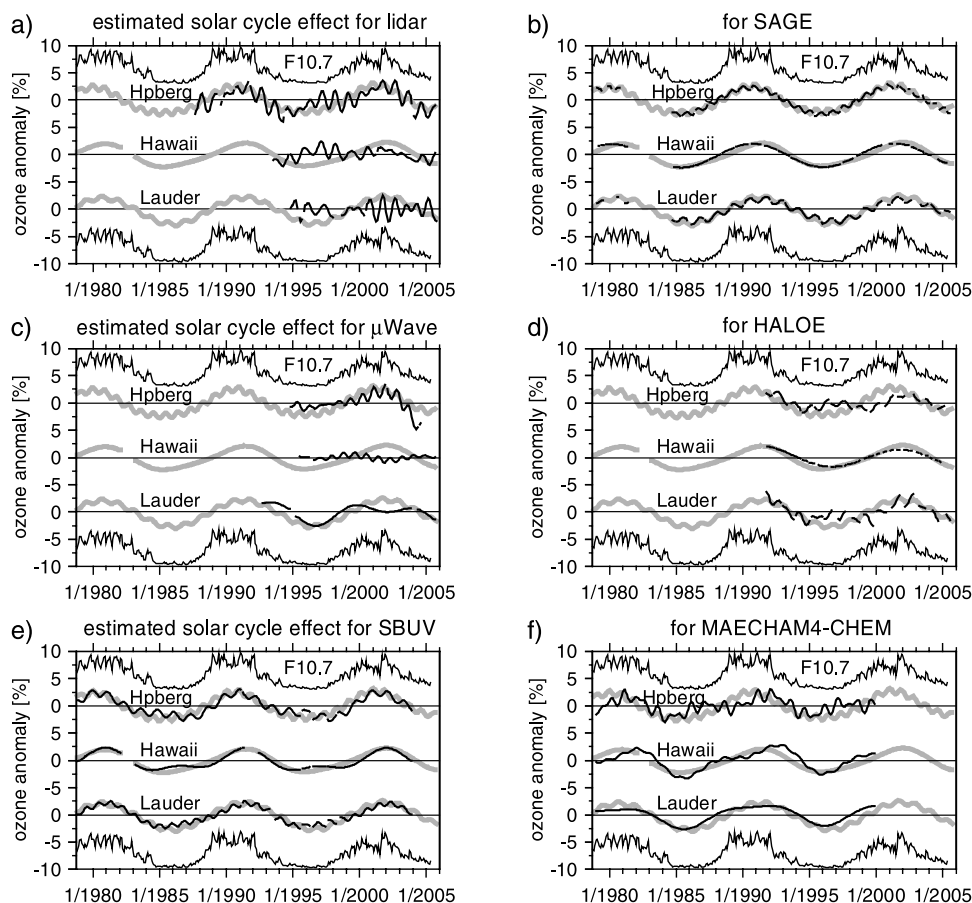
Figure 7. Estimates of ozone anomalies related to the 11-year solar cycle, for three selected stations. Note that the solar cycle estimate is for relative ozone anomalies, averaged from 35 to 45 km altitude. The different panels show results for the different data sets. Results for the all instrument average data set have been underlaid at each station (thick grey line). Thin curves at top and bottom give solar flux at 10.7 cm. Figure 7f compares results for the MAECHAM4-CHEM simulation with the average observed data set.

have been underlaid under the individual instumental records. Note that before the beginning of the lidar, microwave, and HALOE measurements, i.e., usually before 1990, the average record is based on the SAGE and SBUV records only. Also, because SAGE I data before 1982 are often missing, the plotted 5-month running means can be quite close to the SBUV data.

4.1. Instrumental Issues

[26]   In general, all instrumental anomaly records are quite close to the average record. Fluctuations are tracked very similarly by almost all instruments. Correlation coefficients between the individual instrument monthly mean anomalies and the all instrument average anomaly typically range between 0.67 and 0.88. However, due to sampling and instrumental noise, the correlation between the records from two different instruments is usually much lower, only between 0.2 and 0.7. Nevertheless, for the plotted 5 month running means, the individual records are usually within 1 or 2% of the average record. Differences larger than 5% are rare. For the time period after 1995, when almost all instruments have become available, Table 2 gives the standard deviation (1σ) of the individual instrument

monthly anomalies from the all instrument average. These standard deviations have contributions from sampling and instrumental noise. With the exception of the Bordeaux microwave, they range from 1.6% to 4.5%. HALOE, SBUV, and the microwave records at Hawaii and Lauder usually have standard deviations smaller than 3%, whereas SAGE, the lidars, and the Bern microwave have standard deviations larger than 3%. Also, the standard deviations tend to be up to 1% smaller at Hawaii, compared to the midlatitude stations. Since stratospheric variability is generally lower at Hawaii, this indicates that atmospheric variability and sampling errors contribute substantially, at least 1% to the standard deviations. If we assume that the all instrument average is close to the true atmospheric anomaly, Table 2, as well as Figures 4 and 5, indicate that most instruments can measure monthly mean ozone anomalies with an uncertainty better than 4% (1σ).

[27]   While the general agreement between most instruments is quite good, there are some notable differences. At all stations, there seems to be an upward shift in the SBUV data level by about 4% between 1995 and 1998, when the merged data set switches from NOAA 11 to NOAA 9 (http://code916.gsfc.nasa.gov/Data_services/merged/
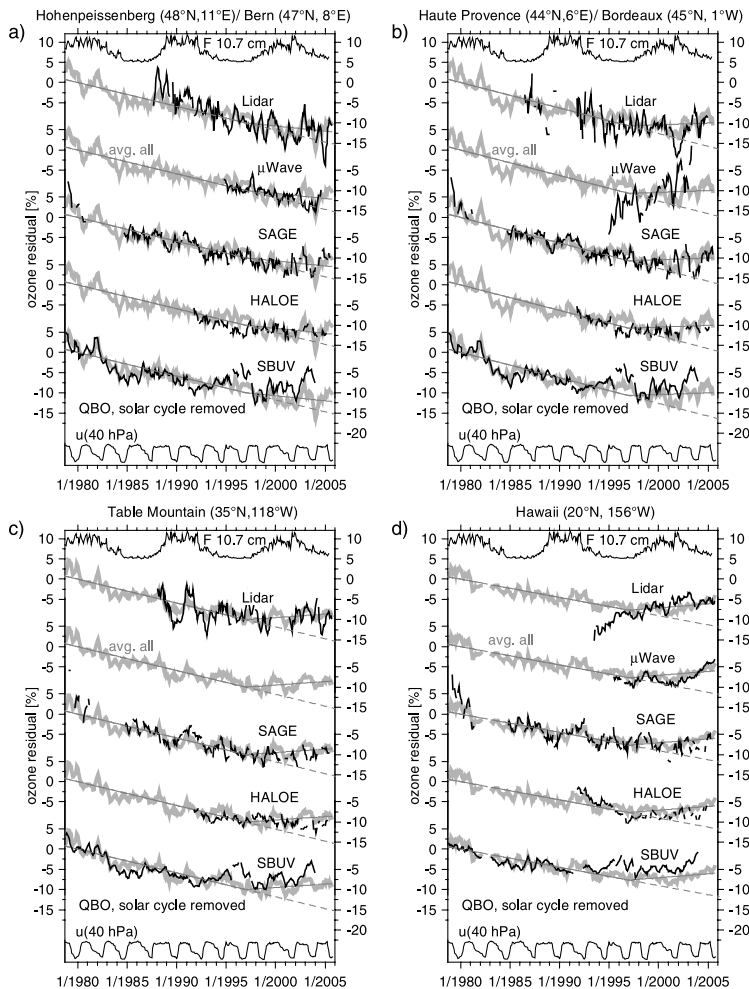
Figure 8. Same as Figure 4, but after subtraction of estimated QBO and solar cycle effects on ozone. The 1997 to 2005 trend line obtained for the average instrumental record by the change of trend term in the regression is also plotted (grey trend line after 1997).
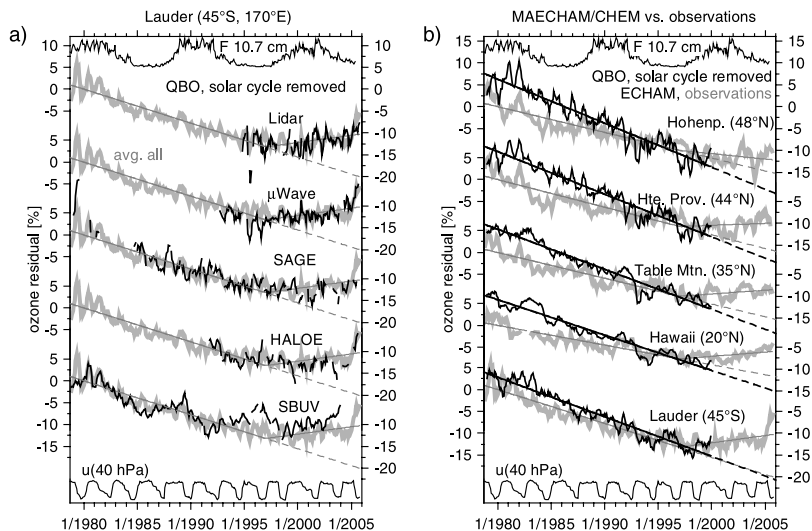

Figure 9. (a) Same as Figure 8, but for the southern mid-latitude station Lauder (New Zealand). (b) Same as Figure 8, but showing the average instrumental and the MAECHAM4-CHEM simulated record at each station, after subtraction of estimated QBO and solar cycle effects on ozone.

Table 2. Instrumental and Sampling Noise as Described by the Standard Deviation (1 σ) of Monthly Mean Differences Between 35 and 45 km Ozone Anomalies Recorded by Each Individual Instrument and the Average Anomalies of All Instruments[a]

Station	Lidar	μWave	SAGE	HALOE	SBUV
Hohenpeissenberg	3.6	3.1	3.5	2.9	2.9
Haute Provence	3.4	8.1	3.1	2.3	2.6
Table Mountain	4.5	–	3.1	2.1	2.5
Hawaii	2.3	1.6	3.1	1.8	2.0
Lauder	3.4	2.8	3.2	3.2	2.7

[a]Standard deviations are given in percent ozone, and are calculated after January 1995 only. Note that the microwave radiometer at Haute Provence/Bordeaux was not included for the average anomaly.

images/sat_coverage.gif). Questions about the consistency of NOAA 9 SBUV/2 with the other SBUV/2 instruments have been raised before, e.g., by *Petropavlovskikh et al.* [2005]. Also, the SBUV data generally show a positive drift compared to the other instruments, both before 1995 and after 1997. The Bordeaux microwave data show an ozone increase throughout their record, that is not observed by the other instruments. This instrumental drift can partly be attributed to a standing wave bias in the observed spectra, which can, however, not account for the total amount of the observed ozone increase. The early Haute Provence lidar data, from 1988 to 1991, or the Lauder lidar data in 1995, show unrealistically low ozone values not recorded by the other instruments. These spurious data as well as the Bordeaux microwave data have been removed from further analysis.

[28] At Hawaii, lidar, SBUV and microwave data show an ozone increase in the last four to five years that is not recorded by SAGE or HALOE. (Note also, that the initial Hawaii lidar data seem to be low before 1996.) However, due to aging and instrumental difficulties, SAGE II (>20 years in orbit!) and HALOE data have become quite sparse in recent years. Table 3 summarizes possible instrumental drifts as measured by linear trends in the differences of each instrument to the average of all instruments. We have separated two periods, up to 1997 where only SBUV,

SAGE, some lidars and HALOE have reasonably long records, and after 1997, where all instruments have data. Here we will only discuss the statistically significant trends (at the 2σ or 95% confidence level), printed in bold in the table. Before 1997, both SAGE and SBUV have significant drifts compared to the instrumental average. SAGE shows a more negative trend than the instrumental average, by about −1.3%/decade, whereas SBUV shows a less negative trend than the average, by about +1.6%/decade. Largely, the instrumental average before 1997 consists of the SAGE and SBUV records only. What is seen in Table 3 then, as well as Figures 4 and 5, is a significant relative drift between these two instruments, or their coordinate systems. Statistically significant pre-1997 drifts are also seen for the Table Mountain lidar and for HALOE at Hawaii.

[29] From 1997 to 2003, SBUV shows quite a large significant drift at Hohenpeissenberg and Haute Provence, by about 5.5% per decade compared to the instrumental average. As mentioned, lidar, microwave and SBUV exhibit a significant positive drift at Hawaii, by about +2.3%/decade, whereas the sparse SAGE and HALOE data both have negative drifts at Hawaii since 1997, by about −3% per decade. The large positive drift of the Bordeaux microwave data has already been mentioned and is a true instrumental problem. The negative drift of the Bern microwave after 1997 is related to the spurious low data from this instrument in 2003. It should probably be ignored. Especially for time periods shorter than about 10 years, we would caution not to over-interpret such drifts, although it is certainly important to monitor them. Larger differences can sometimes be seen for individual instruments and periods up to one or two years, e.g., for the Hohenpeissenberg lidar in 2004/2005, the Table Mountain lidar in 1996 or 2004/2005, or HALOE at Lauder in 2005. The different sampling characteristics, e.g., the infrequent sampling by the solar occultation instruments in summer, and the different vertical coordinates and ozone units used by the various systems (altitude versus pressure, number density versus mixing ratio) likely explain much of these differences.

[30] The most significant drift appears, therefore, between SBUV, which measures ozone mixing ratio versus pressure,

Table 3. Instrumental Drifts as Described by the Trend of Differences Between Monthly Mean 35 to 45 km Ozone Anomalies Recorded by Each Individual Instrument and by the Average of All Instruments[a]

Station	Lidar	μWave	SAGE	HALOE	SBUV
Instrumental Difference Trend (%/Decade) up to Dec 1996					
Hohenpeissenberg	−2.59 ± 3.10		**−1.32 ± 0.84**	−3.37 ± 4.74	**0.95 ± 0.61**
Haute Provence	−0.91 ± 4.06		**−1.26 ± 0.88**	−2.48 ± 4.84	**1.42 ± 0.62**
Table Mountain	**−4.55 ± 2.90**		**−1.47 ± 0.73**	−1.81 ± 3.14	**1.82 ± 0.63**
Hawaii			**−1.24 ± 0.72**	**−3.75 ± 2.65**	**2.10 ± 0.55**
Lauder			−0.68 ± 0.88	−0.52 ± 4.26	**1.92 ± 0.59**
Instrumental Difference Trend (%/Decade) After Jan 1997					
Hohenpeissenberg	−1.24 ± 2.69	**−4.98 ± 2.78**	2.00 ± 3.14	2.26 ± 3.00	**5.99 ± 3.09**
Haute Provence	−1.65 ± 3.10	**15.79 ± 9.45**	−0.54 ± 2.74	0.17 ± 2.51	**5.36 ± 2.49**
Table Mountain	1.99 ± 3.56		−1.18 ± 3.04	−0.40 ± 2.11	−0.27 ± 2.30
Hawaii	**2.94 ± 1.34**	**2.23 ± 1.17**	**−3.95 ± 2.83**	**−2.85 ± 1.62**	2.20 ± 2.08
Lauder	1.79 ± 2.58	1.40 ± 2.09	−0.84 ± 2.80	−1.32 ± 3.20	0.03 ± 2.95

[a]Drifts are in percent ozone per decade and are calculated separately for two periods: up to December 1996; after January 1997. Error bars, given after the plus or minus sign, are 2 standard deviations. Trends significantly different from zero are indicated by bold numbers. Note that before the beginning of the lidar, microwave, and HALOE measurements, i.e., usually before 1990, the average record is based on the SAGE and SBUV records only. At Haute Provence/Bordeaux, the microwave data were not included in the average of all instruments.

Table 4. Ozone Trends From 1979 up to December 1996 for the MAECHAM4-CHEM Simulation[a]

Station	1979 to 1996
Hohenpeissenberg	**−10.07 ± 1.08**
Haute Provence	**−9.76 ± 0.90**
Table Mountain	**−9.16 ± 0.67**
Hawaii	**−8.09 ± 0.76**
Lauder	**−9.04 ± 0.72**

[a]All trends are for the 35 to 45 km altitude range and are given in percent ozone per decade. Error bars, given after the plus or minus sign, are 2 standard deviations. Trends significantly different from zero are indicated by bold numbers. For the error bars, first-order autocorrelation in the regression residuals was accounted for, following the approach described by *Reinsel et al.* [2005].

and SAGE and the other instruments which measure, or can report, ozone number density versus altitude. Since the stratosphere has been cooling in recent decades, pressure surfaces have been moving down to lower altitudes [*Ramaswamy et al.*, 2001]. At altitudes above the ozone peak this means that ozone trends should be larger for fixed altitude levels, than for fixed pressure levels [*Wang et al.*, 1996]. This is seen in Table 3, both before and after 1997: SAGE or the all instrument average on altitude levels have a negative drift in ozone compared to SBUV on pressure levels. SBUV drifts in Table 3 are of the order of +3% per decade against SAGE before 1997. After 1997 they are about +2% to +6% per decade against the all instrument average, albeit with large error bars of 2 to 3% per decade. These drifts are larger than 1 or 2%/decade difference reported by *Li et al.* [2002] or *Rosenfield et al.* [2005] between trends in mixing ratio on pressure levels and trends in number density on altitude levels. The larger drifts reported here seem to indicate an additional instrumental drift for the composite SBUV record. This is consistent with a recent investigation reporting reporting a small drift up to +0.5%/decade for NOAA 11 SBUV/2 ozone against SAGE ozone (converted to mixing ratio versus pressure), over the period 1989 to 2001, and a substantial drift up to +3%/decade for NOAA 16 SBUV/2 against SAGE over the period 2001 to 2003, at the altitudes considered here [*Nazaryan and McCormick*, 2005]. For most instruments, however, the long-term stability seems to be better than ±2.5% per decade. Drifts are usually not significant at the 95% confidence level. The combination of the different instruments should then provide a good representation of the true long-term evolution of ozone in the upper stratosphere, with a long-term stability of 1 or 2%.

[31] Figure 5b compares the ECHAM simulated anomaly record to the average observed record at each station. At all stations, but particularly at the Northern mid-latitude stations, ECHAM simulates a steeper than observed ozone decline. This is most likely caused by the too high upper stratospheric *ClO* concentrations in the model (see discussion of Figure 1). Too much *ClO* gives too much ozone destruction in the upper stratosphere, resulting in too low ozone values, and most likely also in too steep ozone decline. A comparison between the observed and modelled 1979 to 1996 trends is given by Tables 4 and 5. The model overestimates the ozone decline substantially in the Northern Hemisphere, by 3 to 4% per decade, but only slightly by about 1.5% per decade at Lauder. Ozone fluctuations,

however, are tracked quite well by the model simulation after 1985. The large modelled variations before 1985, are not observed by SBUV, the only continous observational record available at that time. Nevertheless both the SBUV data and the ECHAM simulation indicate that the SAGE I data are on a reasonably correct level relative to the SAGE II data [see also *Cunnold et al.*, 2004].

4.2. Ozone Trends and Variations

[32] All anomaly records in Figures 4 and 5 exhibit similar mid- and long-term variations: (1) A long-term declining trend of the order of −4 to −8% per decade. This decline must be attributed to increasing chlorine from anthropogenic sources. (2) A slow fluctuation of the order of 5% peak to peak in phase with the 11-year solar cycle. (3) Shorter time scale variations reaching 5 to over 10% from the QBO, especially in winter. Most of the QBO related peaks occur during or shortly after westerly equatorial zonal winds at 40 hPa. They are seen by all instruments, but not always in the same intensity. Often the station data show a larger amplitude than the zonal mean SAGE and HALOE data. The QBO related fluctuations are more pronounced at the mid-latitude stations, whereas the 11-year solar cycle effect is more visible at the tropical/subtropical station Hawaii. In section 4.3 we give more detailed estimates of the QBO and solar cycle related ozone variations.

[33] Long-term decline and 11-year oscillation combine to a stepwise function that is most obvious at Hawaii. Three periods with nearly constant ozone values, from 1979 to 1982, from 1985 to 1992, and from 1995 to 2005, are separated by two short steep declines, where ozone levels drop by almost 7% over just two or three years. The periods of near-constant ozone correspond to the three increasing phases of the solar cycle, from 1979 to 1982, from 1988 to 1991, and from 1997 to 2002. In these periods, increasing ozone correlated to increasing solar flux seems to have largely compensated decreasing ozone due to increasing destruction by increasing chlorine. However, from 1983 to 1986, and from 1992 to 1996, decreasing ozone correlated to decreasing solar flux and decreasing ozone due to destruction by increasing chlorine have combined to two very steep declines. This stepwise behavior is most visible for the Hawaii model results (Figure 5b), less visible at

Table 5. Observed Ozone Trends up to December 1996, Change of Trend After January 1997, and Resulting Net Ozone Trends After January 1997 at the Different Stations[a]

Station	1979 to 1996	Change After Jan 1997	1997 to 2005
Hohenpeissenberg	**−5.88 ± 0.82**	**3.39 ± 2.65**	−2.49 ± 2.77
Haute Provence	**−6.31 ± 0.92**	**7.20 ± 3.01**	0.89 ± 3.15
Table Mountain	**−5.89 ± 0.73**	**7.62 ± 2.36**	1.73 ± 2.47
Hawaii	**−4.51 ± 0.57**	**6.45 ± 1.80**	**1.94 ± 1.89**
Lauder	**−7.77 ± 0.86**	**11.13 ± 2.74**	**3.35 ± 2.88**

[a]All trends are for the all instrument average and the 35 to 45 km altitude range and are given in percent ozone per decade. Error bars, given after the plus or minus sign, are 2 standard deviations. Trends, and trend changes significantly different from zero are indicated by bold numbers. For the error bars, first-order autocorrelation in the regression residuals was accounted for, following the approach described by *Reinsel et al.* [2005]. Microwave radiometer data from Bordeaux and some spurious low data were excluded.

Table Mountain and Lauder, and almost indistinguishable at Haute Provence and Hohenpeissenberg.

[34] Since about 1996, ozone levels have remained more or less constant at most stations. The more southerly stations even show a distinct increase. At all stations, recent ozone values clearly lie above the extrapolated 1979 to 1996 trend line of the average data record (dashed grey trend line in Figures 4 and 5). Part of this increase must be attributed to the recent solar maximum [*Steinbrecht et al.*, 2004], but part could indicate a slowing down of ozone depletion due to the recent levelling off of stratospheric chlorine. This has been termed "the first stage of a recovery of the ozone layer" [*Newchurch et al.*, 2003]. Some of the most recent data in Figures 4 and 5 show that this "beginning recovery" is still very weak. In fact, Hohenpeissenberg lidar and Bern microwave radiometer report record low ozone values in the winters 2003/2004 and 2004/2005. Very low values are also seen in these two winters at other stations, and by SAGE and HALOE. Such low values have to be expected, since several factors favour low ozone values: Chlorine levels are still high, the solar cycle is near its minimum, and the phase of the QBO in 2004 should also lead to low ozone.

4.3. Estimating and Subtracting QBO and Solar Cycle Effects

[35] Following the approaches of *Newchurch et al.* [2003], and *Steinbrecht et al.* [2004], we now estimate ozone fluctuations related to QBO and 11-year solar cycle. This is done by multiple linear least-squares fitting of appropriate harmonic time series (i.e., sines and cosines) to the observed ozone variations. The fitting procedure also includes a linear trend term, and a change of trend term starting in 1997 [*Reinsel et al.*, 2002, 2005]. While standard procedure assumes that the ozone response looks exactly like a given proxy time series, i.e., equatorial zonal wind at a certain level, or 10.7 cm solar radio flux, fitting harmonic time series allows for additional freedom in the shape of the ozone response. Here we use several harmonics with periods around 29 months to account for the QBO, and two harmonics with periods of 127 and 63 months to account for the 11-year solar cycle. Sidebands generated by an annual cycle modulation of these periods are allowed as well. Note that the attribution of periodicities at 10 and 15 months is ambiguous. These periodicities could come from an annual cycle modulation of the second harmonic of the solar cycle at 63 months, or from the second and third harmonics of the QBO period at about 30 months. Here they were generally minor and have been attributed to the solar cycle in Figure 7. Only statistically significant harmonics are retained by the fitting procedure. See *Newchurch et al.* [2003], *Steinbrecht et al.* [2004], and *Cunnold et al.* [2004] for details about fitting harmonics. See *Reinsel et al.* [2002, 2005] for details about the change of trend term.

[36] The multilinear least squares fits were calculated for all the individual records, as well as for the average anomaly record at each station. Figures 6 and 7 show results for the estimated QBO- and solar cycle related ozone variations, for Hohenpeissenberg/Bern, at northern mid-latitudes, subtropical Hawaii and southern mid-latitude Lauder. Results for Haute Provence/Bordeaux and Table Mountain are similar to those from Hohenpeissenberg, and are not shown. In each

panel the average observed curve for the station has been underlaid (thick grey line). At the mid-latitude stations, the estimated QBO-related ozone variations are of the order of 5 to 10% peak-to-peak. At Hawaii they are smaller, usually less than 5% peak-to-peak [see also *Leblanc and McDermid*, 2001]. QBO variations at Lauder are larger than at Hawaii, but smaller than at the Northern Hemisphere mid-latitude stations. There also seems to be a phase shift between ozone maxima at Hohenpeissenberg, Hawaii, and Lauder. Note that the estimated QBO variations have quite a different shape than the 40 hPa equatorial zonal winds also plotted in Figure 6. QBO-related extrema nearly always occur in winter, in the respective hemispheres. For total column ozone this seasonal synchronization of QBO effects is well known [*Tung and Yang*, 1994a, 1994b]. The spread between the different curves at each station indicates that the uncertainty in the QBO estimate is a few percent at least. With the exception of SBUV, individual instruments tend to show larger variations than seen in the average record. Variations derived from the ECHAM simulation, which includes a nudged QBO, agree quite well with the QBO variation derived from the observations.

[37] Examples for the estimated 11-year solar cycle ozone variations are shown in Figure 7. The derived harmonic solar cycle variation generally follows the 10.7 cm solar radio flux proxy. Ozone is about 5% higher during solar maxima than during solar minima. The magnitude of the solar cycle effect is more or less the same at all stations. The average record does, however, indicate an annual cycle modulation at Hohenpeissenberg and Lauder, which is not apparent at Hawaii. Since annual cycle modulations generally increase at higher latitudes, this seems possible. Results at Haute Provence and Table Mountain are similar to those at Hohenpeissenberg, and are not shown. Note that no reliable estimates can be obtained for those instruments that have time series shorter than 11 to 15 years, i.e., starting after 1993. For the longer time series, however, the agreement between the different estimates at each station is reasonable. The spread between the different estimates is typically less than 2%. Minor differences in phase and amplitude are probably not significant. The solar cycle ozone variation in the ECHAM simulation is quite comparable to the results from the observations.

[38] As pointed out by *Steinbrecht et al.* [2004], it is quite likely that the atmosphere does not react to each solar maximum in the same way. For example, dynamical and transport changes following the major volcanic eruptions of 1982 and 1991, as well as changes in trace gases transported from the lower stratosphere, may have modified the effects of the 1980 and 1991 solar maxima [*Lee and Smith*, 2003]. Different solar maxima may well have resulted in different size ozone maxima. This could have a substantial effect, several percent, on the accuracy of estimated solar cycle ozone variations, which by definition have to follow the prescribed proxy curves, i.e., 10.7 cm solar flux, or in our case a harmonic cosine function.

4.4. Ozone Residual Time Series

[39] Figures 8 and 9 show the ozone time series similar to Figures 4 and 5. However, now the estimated variations due to QBO and solar cycle (from Figures 6 and 7) have been subtracted. For those instruments with time series shorter

than 11 years, the solar cycle estimate for the average of all instruments was subtracted. We call the remaining variations "ozone residuals". They are our best representation of ozone changes due to influences other than QBO and solar cycle, i.e., largely due to changing chlorine levels. A "beginning recovery of the ozone layer" would manifest itself by ozone residuals that are leveling off, or even increasing in recent years. At least, ozone residuals should lie clearly above the extrapolated 1979 to 1996 trend line (dashed grey line in Figures 8 and 9).

[40] Figures 8 and 9 show clear evidence for such a "beginning recovery" above Lauder in the Southern Hemisphere (Figure 9a), and somewhat less clear evidence for Hawaii (Figure 8d), Table Mountain (Figure 8c) and Haute Provence (Figure 8b). For the most northerly station Hohenpeissenberg/Bern, however, a "beginning recovery" is much less obvious (Figure 8a). Due to very low values in the winters 2003/2004 and 2004/2005, the recent data at Hohenpeissenberg/Bern are not significantly above the trend line. To a lesser degree, low values in these two winters are also recorded at Table Mountain and Haute Provence.

[41] A more quantitative description is given in Table 5, which reports ozone trends and uncertainties obtained for the all instrument average data set. Upper stratospheric ozone trends before 1997 were about −6%/decade at the northern mid-latitude stations, almost −8%/decade at Lauder in southern mid-latitudes, and only −4.5%/decade at subtropical Hawaii. Similar interhemispheric and latitudinal differences have been reported, e.g., by *Li et al.* [2002] or *Rosenfield et al.* [2005]. After the assumed January 1997 turning point, Table 5 indicates a significant change of the trend at all stations. This change in trend is largest at Lauder, where it reaches +11%/decade. Trend changes of around +7% are found at Haute Provence, Table Mountain and Hawaii. Error bars for these trend changes are about 2 to 3%/decade (2σ or 95% uncertainty level), and are roughly the same size at all stations. However, a much smaller and therefore less significant trend change by only +3.4%/decade is found at Hohenpeissenberg/Bern. This is consistent with the visual impression from Figure 8. Hohenpeissenberg/Bern is also the only station that still shows a negative ozone trend after 1997, albeit insignificant, whereas the other northern stations show (insignificant) positive ozone trends after 1997. Lauder even shows a significant positive ozone trend after 1997. Both the negative ozone trend before 1997, and the change of trend after 1997 are largest above southern mid-latitude Lauder. The large change from Haute Provence to Hohenpeissenberg is, however, surprising and should be investigated in the future.

[42] One factor might be the timing of a beginning recovery. A later beginning at higher latitudes has to be expected from age of stratospheric air studies [*Waugh and Hall*, 2002]. These studies indicate that air at 40 km altitude, 50°N (i.e., Hohenpeissenberg/Bern) is about 2 years older than air at 20° (i.e., Hawaii). This means that a beginning "ozone recovery" should appear at Hawaii about 2 years earlier than at Hohenpeissenberg, and might therefore be less clear at Hohenpeissenberg. This is roughly consistent with Figures 8 and 9, which seem to indicate a change of trend point around 1997/1998 for Table Mountain and Hawaii, but a later point around 2001/2002 for Haute

Provence and Hohenpeissenberg. This timing difference, however, has been ignored in our change of trend calculations, which use a fixed turning point in January 1997. Contrary to *Waugh and Hall* [2002], which give similar age of air for northern and southern mid-latitudes, Lauder at 45° southern latitude indicates a much earlier "beginning recovery" than Hohenpeissenberg/Bern at 48° northern latitude. Furthermore, despite the higher latitude, the ozone record above Lauder indicates an earlier "beginning recovery" than seen at low-latitude Hawaii.

[43] Another relevant aspect might be higher meteorological variability at Hohenpeissenberg/Bern: Meteorological variability is higher in the Northern Hemisphere, because planetary wave activity is higher and stratospheric mid-winter warmings occur frequently. Polar, or tropical, air-masses are more likely to appear at mid-latitudes. In the Southern Hemisphere planetary wave activity is lower and stratospheric mid-winter warmings are very rare. This higher meteorological "noise" might mask a "beginning recovery" signal at Hohenpeissenberg, and Haute Provence, while the same signal can be seen clearly in the "less noisy" stratosphere above Hawaii or Lauder. It still leaves the question, why the recovery seems to begin earlier at southern mid-latitude Lauder than at near-tropical Hawaii.

[44] Note that temperature changes, whether due to increasing CO_2 cooling or due to changes in the frequency of stratospheric warmings, will also affect ozone in the upper stratosphere. Based on 2-D model calculations, *Rosenfield et al.* [2002] report that upper stratospheric cooling due to increasing CO_2 levels could raise ozone levels by 2 to 3%. This effect is due to a slowdown of ozone loss cycles at lower temperatures. In the upper stratosphere, increasing CO_2 cooling would, therefore, speed up ozone recovery and would result in a more pronounced increase of ozone levels. The effect might differ between Lauder and Northern Hemisphere stations, if temperature changes are different in the two hemispheres. Interhemispheric differences in Cl_y partitioning [*Considine et al.*, 1998; *Li et al.*, 2002; *Rosenfield et al.*, 2005] might also play a role. According to *Newchurch et al.* [2003], however, temperature changes have been small and have contributed very little to the levelling off of ozone values since about 1997. Nevertheless, questions related to long-term temperature changes are important and deserve a detailed investigation in the future.

5. Summary

[45] We have investigated main characteristics of long-term monitoring of upper stratospheric ozone, carried out by ground-based lidars and microwave radiometers within the Network for the Detection of Stratospheric Change, and by several satellite instruments. Climatological mean differences between lidars, microwave radiometers, SAGE and HALOE are usually smaller than 5% between 30 and 45 km altitude. Significant bias larger than 5% is seen at some lidar stations and at altitudes above 40 km. To a substantial degree it is attributed to the processing algorithms used at the individual stations. Note that such systematic biases may be corrected in future data releases.

[46] Nearly all instruments show a very similar evolution of upper stratospheric ozone over the last 10 to 25 years.

Many features of the observed evolution are reproduced quite well by the 1979 to 1999 period from simulation by the MAECHAM4-CHEM chemistry climate model. However, in the upper stratosphere the model shows too low ozone values and too large ozone decline, probably to an underestimation of methane and a consequent overestimation of ClO. Ozone anomalies from the different observations and from the model, averaged with a 5-month boxcar, typically agree within a few percent. The combined SBUV data set used here seems to have an upward shift by about 3% from 1995 to 1998, when the merged data set switches from NOAA 11 SBUV/2 to NOAA 9 SBUV/2 [see also *Petropavlovskikh et al.*, 2005]. The combined SBUV record, in mixing ratio versus pressure coordinates, shows a drift of about 2% per decade compared to the other records, which are in number density versus altitude coordinates. Cooling of the stratosphere should have lead to a shift between these different coordinate systems, and could explain a good fraction of this drift, but not all of it. Differences larger than 3% to 5% are sometimes seen for individual instruments/stations over periods of one or two years. The quite different sampling characteristics of the various instruments are likely to contribute substantially to such differences. The combination of all instruments, however, provides a very consistent picture of the long-term evolution of ozone in the upper stratosphere, with a long-term stability better than about 2%.

[47] In the next years, a switchover from aging satellite instruments like SAGE II and HALOE to newer instruments like SCIAMACHY, GOMOS, SAGE III, MIPAS, MLS, OMI, and others will take place. The combination of ground-based NDSC lidars and microwave radiometers can provide a stable reference for the transition to this next generation of satellite based ozone monitoring instruments.

[48] Upper stratospheric ozone shows three main variations: First, the QBO modulates ozone on the time scale of two to three years, with ozone changes of the order of 5 to 10%, particularly in winter. Second, a long-term ozone variation of about 5% peak to valley is related to the 11-year solar cycle. Third, ozone in the upper stratosphere has seen a long-term decline by 10 to 15% since 1980. This decline is caused by chemical destruction through chlorine from man-made sources [*Crutzen*, 1974; *Molina and Rowland*, 1974]. Following the 1987 Montreal Protocol, chlorine seems to have peaked at some time between 1997 and 2002 in the upper stratosphere [*WMO*, 2003]. Ozone levels seem to be following the recent chlorine turnaround, and at many stations the previously steep ozone decline has not continued in the last five years. This seems to indicate a beginning recovery of the ozone layer. However, it is difficult to unambiguously separate ozone changes due to chlorine changes in recent years from effects of the recent maximum of the 11-year solar cycle. Also, chlorine is still near its maximum and is not expected to return to pre-1980 levels before 2050 [*Engel et al.*, 2002; *WMO*, 2003]. Therefore, a beginning recovery is still weak and record low upper stratospheric ozone values have been observed at northern mid-latitude stations in the winters 2003/2004 and 2004/2005. Effects of changing stratospheric temperatures [*Rosenfield et al.*, 2002] and changes in the Brewer-Dobson circulation [*Salby et al.*, 2002] may be important and should be investigated.

References

Anderson, J., J. M. Russell III, S. Solomon, and L. E. Deaver (2000), HALOE confirmation of stratospheric chlorine decreases in accordance with the Montreal Protocol, *J. Geophys. Res.*, *105*, 4483–4490.

Austin, J., et al. (2003), Uncertainties and assessments of chemistry-climate models of the stratosphere, *Atmos. Chem. Phys.*, *3*, 1–27.

Bhartia, P. K., R. D. McPeters, C. L. Mateer, L. E. Flynn, and C. Wellemeyer (1996), Algorithm for the estimation of vertical ozone profile from the backscattered ultraviolet (BUV) technique, *J. Geophys. Res.*, *101*, 18,793–18,806.

Brasseur, G., and S. Solomon (1984), *Aeronomy of the Middle Atmosphere*, 441 pp., Springer, New York.

Brinksma, E. J., J. Ajtic, J. B. Bergwerff, G. E. Bodeker, I. S. Boyd, J. F. de Haan, W. Hogervorst, J. W. Hovenier, and D. P. J. Swart (2002), Five years of observations of ozone profiles over Lauder, New Zealand, *J. Geophys. Res.*, *107*(D14), 4216, doi:10.1029/2001JD000737.

Calisesi, Y., H. Wernli, and N. Kämpfer (2001), Midstratospheric ozone variability over Bern related to planetary wave activity during the winters 1994–1995 to 1998–1999, *J. Geophys. Res.*, *106*, 7903–7916.

Claude, H., F. Schönenborn, W. Steinbrecht, and W. Vandersee (1994), New evidence for ozone depletion in the upper stratosphere, *Geophys. Res. Lett.*, *21*, 2409–2412.

Connor, B. J., A. Parrish, J. J. Tsou, and M. P. McCormick (1995), Error analysis for the ground-based microwave ozone measurements during STOIC, *J. Geophys. Res.*, *100*, 9283–9291.

Considine, D. B., A. E. Dessler, C. H. Jackman, J. E. Rosenfield, P. E. Meade, M. R. Schoeberl, A. E. Roche, and J. W. Waters (1998), Interhemispheric asymmetry in the 1 mbar O3 trend: An analysis using an interactive zonal mean model and UARS data, *J. Geophys. Res.*, *103*, 1607–1618.

Crutzen, P. J. (1974), Estimates of possible future ozone reductions from continued use of fluoro-chloro-methanes CF_2Cl_2, $CFCl_3$, *Geophys. Res. Lett.*, *1*, 205–208.

Cunnold, D. M., E.-S. Yang, M. J. Newchurch, G. C. Reinsel, J. M. Zawodny, and J. M. Russell III (2004), Comment on "Enhanced upper stratospheric ozone: Sign of recovery or solar cycle effect?" by W. Steinbrecht et al., *J. Geophys. Res.*, *109*, D14305, doi:10.1029/2004JD004826.

DeBacker, H., E. P. Visser, D. DeMuer, and D. P. J. Swart (1994), Potential for meteorological bias in lidar ozone data sets resulting from the restricted frequency of measurement due to cloud cover, *J. Geophys. Res.*, *99*, 1395–1401.

Douglass, A. E., R. B. Rood, and R. S. Stolarski (1985), Interpretation of Ozone Temperature Correlations: 2. Analysis of SBUV Ozone Data, *J. Geophys. Res.*, *90*, 10,693–10,708.

Engel, A., M. Strunk, M. Müller, H.-P. Haase, C. Poss, I. Levin, and U. Schmidt (2002), The temporal development of total chlorine in the high latitude stratosphere based on reference distributions of mean age derived from CO_2 and SF_6, *J. Geophys. Res.*, *107*(D12), 4136, doi:10.1029/2001JD000584.

Frith, S., R. S. Stolarski, and P. K. Bhartia (2004), Implications of version 8 TOMS and SBUV data for long-term trend analysis, in *Proceedings of XX Quadrennial Ozone Symposium, June 2004, Kos, Greece*, edited by C. S. Zerefos, pp. 65–66, Univ. of Athens, Athens, Greece.

Giorgetta, M. A., and L. Bengtsson (1999), The potential role of the quasi-biennial oscillation in the stratosphere-troposphere exchange as found in water vapour in general circulation model experiments, *J. Geophys. Res.*, *104*, 6003–6019.

Godin, S., et al. (1999), Differential Absorption Ozone Lidar Algorithm Intercomparison, *Appl. Opt.*, *38*, 6225–6236.

Godin-Beekmann, S., J. Porteneuve, and A. Garnier (2003), Systematic DIAL lidar monitoring of the stratospheric ozone vertical distribution at Observatoire de Haute-Provence (43.92°N, 5.71°E), *J. Environ. Monit.*, *5*, 57–67, doi:10.1039/b205880d.

Guirlet, M., P. Keckhut, S. Godin, and G. Mégie (2000), Description of the long-term ozone data series obtained from different instrumental techniques at a single location: The Observatoire de Haute-Provence (43.9°N, 5.7°E), *Ann. Geophys.*, *18*, 1325–1339.

Heath, D. F., A. J. Krueger, H. A. Roeder, and B. D. Henderson (1975), The Solar Backscatter Ultraviolet and Total Ozone Mapping Spectrometer (SBUV/TOMS) for Nimbus 6, *Opt. Eng.*, *14*, 323–331.

Hilsenrath, E., R. P. Cebula, M. T. Deland, K. Laamann, S. Taylor, C. Wellemeyer, and P. K. Bhartia (1995), Calibration of the NOAA-11 Solar Backscatter Ultraviolet (SBUV/2) Ozone Data Set from 1989 to 1993 using In-Flight Calibration Data and SSBUV, *J. Geophys. Res.*, *100*, 1351–1366.

Hood, L. L., J. L. Jirikowic, and J. P. McCormack (1993), Quasi-decadal variability of the stratosphere: Influence of long-term solar ultraviolet variations, *J. Atmos. Sci.*, *50*, 3941–3958.

Huang, F. T., C. A. Reber, and J. Austin (1997), Ozone diurnal variations observed by UARS and their model simulation, *J. Geophys. Res.*, *102*, 12,971–12,986.

Jackman, C. H., E. L. Fleming, F. M. Vitt, and D. B. Considine (1999), The influence of solar proton events on the ozone layer, *Adv. Space Res.*, *24*, 625–630.

Kämpfer, N. (1995), Microwave remote sensing of the atmosphere in Switzerland, *Opt. Eng.*, *34*, 2413–2424.

Keckhut, P., et al. (2004), Review of ozone and temperature lidar validations performed within the framework of the Network for the Detection of Stratospheric Change, *J. Environ. Monit.*, *6*, 721–733, doi:10.1039/b404256e.

Leblanc, T., and I. S. McDermid (2000), Stratospheric ozone climatology from lidar measurements at Table Mountain (34.4°N, 117.7°W) and Mauna Loa (19.5°N, 155.6°W), *J. Geophys. Res.*, *105*, 14,613–14,624.

Leblanc, T., and I. S. McDermid (2001), Quasi-biennial oscillation signatures in ozone and temperature observed by lidar at Mauna Loa, Hawaii (19.5°N, 155.6°W), *J. Geophys. Res.*, *106*, 14,869–14,874.

Lee, H., and A. K. Smith (2003), Simulation of the combined effects of solar cycle, quasi-biennial oscillation, and volcanic forcing on stratospheric ozone changes in recent decades, *J. Geophys. Res.*, *108*(D2), 4049, doi:10.1029/2001JD001503.

Li, J., D. M. Cunnold, H.-J. Wang, E.-S. Yang, and M. J. Newchurch (2002), A discussion of upper stratospheric ozone asymmetries and SAGE trends, *J. Geophys. Res.*, *107*(D23), 4705, doi:10.1029/2001JD001398.

Manzini, E., and N. A. McFarlane (1998), The effect of varying the source spectrum of a gravity wave parameterization in a middle atmosphere general circulation model, *J. Geophys. Res.*, *103*, 31,523–31,539.

Manzini, E., B. Steil, C. Brühl, M. A. Giorgetta, and K. Krger (2003), A new interactive chemistry-climate model: 2. Sensitivity of the middle atmosphere to ozone depletion and increase in greenhouse gases: Implications for recent stratospheric cooling, *J. Geophys. Res.*, *108*(D14), 4429, doi:10.1029/2002JD002977.

McCormick, M. P., J. M. Zawodny, R. E. Veiga, J. C. Larsen, and P. H. Wang (1989), An Overview Of SAGE I And II Ozone Measurements, *Planet. Space Sci.*, *37*, 1567–1586.

McDermid, I. S., S. M. Godin, and L. O. Lindqvist (1990), Ground-based laser DIAL system for long-term measurements of stratospheric ozone, *Appl. Opt.*, *29*, 3603–3612.

McDermid, I. S., et al. (1998), OPAL: Network for the detection of stratospheric change ozone profiler assessment at Lauder, New Zealand: 2. Intercomparison of revised results, *J. Geophys. Res.*, *103*, 28,693–28,700.

McPeters, R. D., et al. (1999), Results from the 1995 stratospheric ozone profile intercomparison at Mauna Loa, *J. Geophys. Res.*, *104*, 30,505–30,514.

Meijer, Y. J., R. J. van der A, R. F. van Oss, D. P. J. Swart, H.M. Kelder, and P. V. Johnston (2003), Global Ozone Monitoring Experiment ozone profile characterization using interpretation tools and lidar measurements for intercomparison, *J. Geophys. Res.*, *108*(D23), 4723, doi:10.1029/2003JD003498.

Molina, M. J., and F. S. Rowland (1974), Stratospheric sink for chlorofluoromethanes - chlorine atom catalyzed destruction of ozone, *Nature*, *249*, 810–812.

Morris, G. A., J. F. Gleason, J. M. Russell III, M. R. Schoeberl, and M. P. McCormick (2002), A comparison of HALOE V19 with SAGE II V6.00 ozone observations using trajectory mapping, *J. Geophys. Res.*, *107*(D13), 4177, doi:10.1029/2001JD000847.

Nazaryan, H., and M. P. McCormick (2005), Comparisons of Stratospheric Aerosol and Gas Experiment (SAGE II) and Solar Backscatter Ultraviolet Instrument (SBUV/2) ozone profiles and trend estimates, *J. Geophys. Res.*, *110*, D17302, doi:10.1029/2004JD005483.

Nazaryan, H., M. P. McCormick, and J. M. Russell III (2005), New studies of SAGE II and HALOE ozone profile and long-term change comparisons, *J. Geophys. Res.*, *110*, D09305, doi:10.1029/2004JD005425.

Newchurch, M. J., E.-S. Yang, D. M. Cunnold, G. C. Reinsel, J. M. Zawodny, and J. M. Russell III (2003), Evidence for slowdown in stratospheric ozone loss: First stage of ozone recovery, *J. Geophys. Res.*, *108*(D16), 4507, doi:10.1029/2003JD003471.

Parrish, A., B. J. Connor, J. J. Tsou, I. S. McDermid, and W. P. Chu (1992), Ground-based microwave monitoring of stratospheric ozone, *J. Geophys. Res.*, *97*, 2541–2546.

Pelon, J., and G. Mégie (1982), Ozone monitoring in the troposphere and lower stratosphere: Evaluation and operation of a ground-based lidar station, *J. Geophys. Res.*, *87*, 4947–4955.

Petropavlovskikh, I., C. Ahn, P. K. Bhartia, and L. E. Flynn (2005), Comparison and covalidation of ozone anomalies and variability observed in SBUV(/2) and Umkehr northern midlatitude ozone profile estimates, *Geophys. Res. Lett.*, *32*, L06805, doi:10.1029/2004GL022002.

Ramaswamy, V., et al. (2001), Stratospheric temperature trends: Observations and model simulations, *Rev. Geophys.*, *39*, 71–122.

Randeniya, L. K., P. F. Vohralik, and I. C. Plumb (2002), Stratospheric ozone depletion at northern mid latitudes in the 21 st century: The importance of future concentrations of greenhouse gases nitrous oxide and methane, *Geophys. Res. Lett.*, *29*(4), 1051, doi:10.1029/2001GL014295.

Rayner, N. A., D. E. Parker, E. B. Horton, C. K. Folland, L. V. Alexander, D. P. Rowell, E. C. Kent, and A. Kaplan (2003), Global analyses of sea surface temperature, sea ice, and night marine air temperature since the late nineteenth century, *J. Geophys. Res.*, *108*(D14), 4407, doi:10.1029/2002JD002670.

Reinsel, G. C., E. C. Weatherhead, G. C. Tiao, A. J. Miller, R. M. Nagatani, D. J. Wuebbles, and L. E. Flynn (2002), On detection of turnaround and recovery in trend for ozone, *J. Geophys. Res.*, *107*(D10), 4078, doi:10.1029/2001JD000500.

Reinsel, G. C., A. J. Miller, E. C. Weatherhead, L. E. Flynn, R. M. Nagatani, G. C. Tiao, and D. J. Wuebbles (2005), Trend analysis of total ozone data for turnaround and dynamical contributions, *J. Geophys. Res.*, *110*, D16306, doi:10.1029/2004JD004662.

Rinsland, C. P., et al. (2003), Long-term trends of inorganic chlorine from ground-based infrared solar spectra: Past increases and evidence for stabilization, *J. Geophys. Res.*, *108*(D8), 4252, doi:10.1029/2002JD003001.

Rosenfield, J. E., A. R. Douglass, and D. B. Considine (2002), The impact of increasing carbon dioxide on ozone recovery, *J. Geophys. Res.*, *107*(D6), 4049, doi:10.1029/2001JD000824.

Rosenfield, J. E., S. M. Frith, and R. S. Stolarski (2005), Version 8 SBUV ozone profile trends compared with trends from a zonally averaged chemical model, *J. Geophys. Res.*, *110*, D12302, doi:10.1029/2004JD005466.

Russell, J. M., III, L. L. Gordley, J. H. Park, S. R. Drayson, W. D. Hesketh, R. J. Cicerone, A. F. Tuck, J. E. Frederick, J. E. Harris, and P. J. Crutzen (1993), The Halogen Occultation Experiment, *J. Geophys. Res.*, *98*, 10,777–10,798.

Salby, M., P. Callaghan, P. Keckhut, S. Godin, and M. Guirlet (2002), Interannual changes of temperature and ozone: Relationship between the lower and upper stratosphere, *J. Geophys. Res.*, *107*(D18), 4342, doi:10.1029/2001JD000421.

Schneider, N., O. Lezeaux, J. de La Noë, J. Urban, and P. Ricaud (2003), Validation of ground-based observations of stratomesospheric ozone, *J. Geophys. Res.*, *108*(D17), 4540, doi:10.1029/2002JD002925.

Schneider, N., F. Selsis, J. Urban, O. Lezeaux, J. La Noë, and P. Ricaud (2005), Seasonal and diurnal ozone variations: Observations and modeling, *J. Atmos. Chem.*, *50*, 25–47, doi:10.1007/s10874-005-1172-z.

SPARC (1998), Assessment of trends in the vertical distribution of ozone, edited by N. Harris, R. Hudson, and C. Phillips, *SPARC Rep. 1*, World Clim. Res. Programme, Geneva. (Available at http://www.atmosp.physics.utoronto.ca/SPARC/SPARCReport1)

Steil, B., C. Brühl, E. Manzini, P. J. Crutzen, J. Lelieveld, P. J. Rasch, E. Roeckner, and K. Krüger (2003), A new interactive chemistry climate model: 1. Present day climatology and interannual variability of the middle atmosphere using the model and 9 years of HALOE/UARS data, *J. Geophys. Res.*, *108*(D9), 4290, doi:10.1029/2002JD002971.

Steinbrecht, W., P. Winkler, and H. Claude (1997), Ozon- und Temperaturmessungen mittels Lidar am Hohenpeissenberg, *Rep. 200*, Deutscher Wetterdienst, Offenbach, Germany. (Available at http://www.dwd.de/de/FundE/Observator/MOHp/hp2/ozon/pubs_as_pdf/dwd_200.pdf)

Steinbrecht, W., H. Claude, U. Köhler, and K. P. Hoinka (1998), Correlations between tropopause height and total ozone: Implications for long-term changes, *J. Geophys. Res.*, *103*, 19,183–19,192.

Steinbrecht, W., H. Claude, and P. Winkler (2004), Enhanced upper stratospheric ozone: Sign of recovery or solar cycle effect?, *J. Geophys. Res.*, *109*, D02308, doi:10.1029/2003JD004284.

Timmreck, C., H.-F. Graf, and B. Steil (2004), Aerosol chemistry interactions after the Mt. Pinatubo eruption, in *Volcanism and the Earth's Atmosphere*, *Geophys. Monogr. Ser.*, vol. 139, edited by A. Robock and C. Oppenheimer, pp. 213–225, AGU, Washington, D. C.

Tourpali, K., C. J. E. Schuurmans, R. van Dorland, B. Steil, and C. Brühl (2003), Stratospheric and tropospheric response to enhanced solar UV-radiation: A model study, *Geophys. Res. Lett.*, *30*(5), 1231, doi:10.1029/2002GL016650.

Tsou, J. J., B. J. Connor, A. Parrish, R. B. Pierce, I. S. Boyd, G. E. Bodeker, W. P. Chu, J. M. Russell III, D. P. J. Swart, and T. J. McGee (2000), NDSC millimeter wave ozone observations at Lauder, New Zealand,

1992–1998: Improved methodology, validation, and variation study, *J. Geophys. Res.*, *105*, 24,263–24,281.

Tung, K. K., and H. Yang (1994a), Global QBO in circulation and ozone. Part I: Reexamination of observational evidence, *J. Atmos. Sci.*, *51*, 2699–2707.

Tung, K. K., and H. Yang (1994b), Global QBO in circulation and ozone. Part II: A simple mechanistic model, *J. Atmos. Sci.*, *51*, 2708–2721.

Wang, H. J., D. M. Cunnold, and X. Bao (1996), A critical analysis of SAGE ozone trends, *J. Geophys. Res.*, *101*, 12,495–12,514.

Wang, H. J., D. M. Cunnold, L. W. Thomason, J. M. Zawodny, and G. E. Bodeker (2002), Assessment of SAGE version 6.1 ozone data quality, *J. Geophys. Res.*, *107*(D23), 4691, doi:10.1029/2002JD002418.

Waugh, D. W., and T. M. Hall (2002), Age of stratospheric air: Theory, observations, and models, *Rev. Geophys.*, *40*(4), 1010, doi:10.1029/2000RG000101.

Werner, J., K. W. Rothe, and H. Walther (1983), Monitoring of the stratospheric ozone layer by laser radar, *Appl. Phys. B*, *32*, 113–118.

World Meteorological Organization (WMO) (1999), Scientific assessment of ozone depletion: 1998, *Rep. 44*, Geneva, Switzerland.

World Meteorological Organization (WMO) (2003), Scientific assessment of ozone depletion: 2002, *Rep. 47*, Geneva, Switzerland.

Zawodny, J. M., and M. P. McCormick (1991), Stratospheric Aerosol and Gas Experiment II measurements of the quasi-biennial oscillation in ozone and nitrogen dioxide, *J. Geophys. Res.*, *96*, 9371–9377.

————————

P. K. Bhartia, S. M. Hollandsworth-Frith, and R. S. Stolarski, NASA GSFC, Greenbelt, MD 20771, USA.

G. E. Bodeker and B. J. Connor, NIWA, Omakau, Central Otago, New Zealand.

I. S. Boyd, NIWA-ERI, Ann Arbor, MI 48108, USA.

C. Brühl and B. Steil, Max-Planck-Institute for Chemistry, D-55028 Mainz, Germany.

Y. Calisesi, International Space Science Institute, CH-3012 Bern, Switzerland.

H. Claude, F. Schönenborn, and W. Steinbrecht, Meteorological Observatory Hohenpeissenberg, German Weather Service, Albin Schwaiger Weg 10, D-82383 Hohenpeissenberg, Germany. (hans.claude@dwd.de; wolfgang.steinbrecht@dwd.de)

J. de la Noë and N. Schneider, OASU/L3AB, Université Bordeaux 1, CNRS-INSU, F-33270 Floirac, France.

M. A. Giorgetta, Max-Planck-Institute for Meteorology, D-20146 Hamburg, Germany.

S. Godin and T. Song, CNRS Service d'Aeronomie, F-75004 Paris, France.

K. Hocke and N. Kämpfer, Institute of Applied Physics, University of Bern, CH-3012 Bern, Switzerland.

T. Leblanc and I. S. McDermid, Table Mountain Facility, NASA-JPL, Wrightwood, CA 92397, USA.

E. Manzini, Istituto Nazionale di Geofisica e Vulcanologia, I-40128 Bologna, Italy.

M. P. McCormick and J. M. Russell III, Hampton University, Hampton, VA 23668, USA.

Y. J. Meijer and D. P. J. Swart, RIVM, NL-3720 Bilthoven, Netherlands.

A. D. Parrish, Astronomy Department, University of Massachusetts, Amherst, MA 01003, USA.

L. W. Thomason and J. M. Zawodny, NASA LARC, Hampton, VA 23681, USA.